Proceedings World Geothermal Congress 2026
Calgary, Canada, June 8 – 11, 2026

Corrosion Risk Assessment for Reinjection of Combined Brine to Intermediate Aquifer

Sigit Prabowo[1]*, Keith Lichti[1], Soroor Ghaziof[1], Kelly Melia[2], Farrell Siega[2], and Aimee Calibugan[3]
Quest Integrity, 20 Somme Road, Upper Hutt 5018, New Zealand[1]*, Mercury New Zealand Limited, 283 Vaughan Road, Rotorua 3010, New Zealand[2],
Jacobs, Carlaw Park 12-16 Nicholls Lane, Level 2. Parnell Auckland 1010, New Zealand[3]
S.Prabowo@questintegrity.com

Keywords: Reinjection, Rotokawa, geothermal, intermediate aquifer, casing corrosion

ABSTRACT

The Rotokawa geothermal field in New Zealand has an intermediate aquifer that is known to be corrosive to carbon steel well casings and cements. The chemistry of the intermediate aquifer contains corrosive CO_2-rich fluids which comes from the arising CO_2 gas from deep reservoir fluids through the permeable features of the intermediate aquifer. A combined brine (mixed brine and condensate from a binary plant) has been reinjected to dilute the corrosive fluid within the intermediate aquifer. However, the reinjection of combined brine can also increase the partial pressure of CO_2 which may increase the corrosivity of the intermediate aquifer fluid. This paper investigates the impact of reinjecting combined brine fluids from several wells on the corrosion of carbon steel casing of the nearby wells using theoretical analysis. We first construct Pourbaix diagrams to predict the stability regions of corrosion products, followed by CO_2 corrosion rate predictions based on the formation of these products. The procedures used for this assessment and the corrosion risk for nearby well casings are described. The results show that the presence of H_2S within the fluid is a critical factor for controlling CO_2 corrosion of carbon steel casing at the nearby wells.

1 INTRODUCTION

The Rotokawa Geothermal Field is located near Taupō in the North Island of New Zealand. It supports two geothermal power stations: the Rotokawa Power Station and the Ngā Awa Pūrua (NAP) Power Station. The Rotokawa Power Station is a binary plant that has been in operation since 1997, while the NAP Power Station is a flash plant that has been in operation since 2010. The Rotokawa Geothermal Field has an intermediate aquifer that is known to be corrosive to cement and well casings. Figure 1 illustrates the simulated mass balance of the intermediate aquifer in its natural state. Here, the intermediate aquifer chemistry is generated by a complex interaction of multiple geothermal fluid sources, which is a mix of permeated fluid flow from the deeper reservoir and crossflow within the field. The permeation of fluid from the deep reservoir into the intermediate aquifer's results in a mixed fluid that is depleted in H_2S and enriched in CO_2. This CO_2-rich fluid is corrosive to the cements and casings used in geothermal wells.

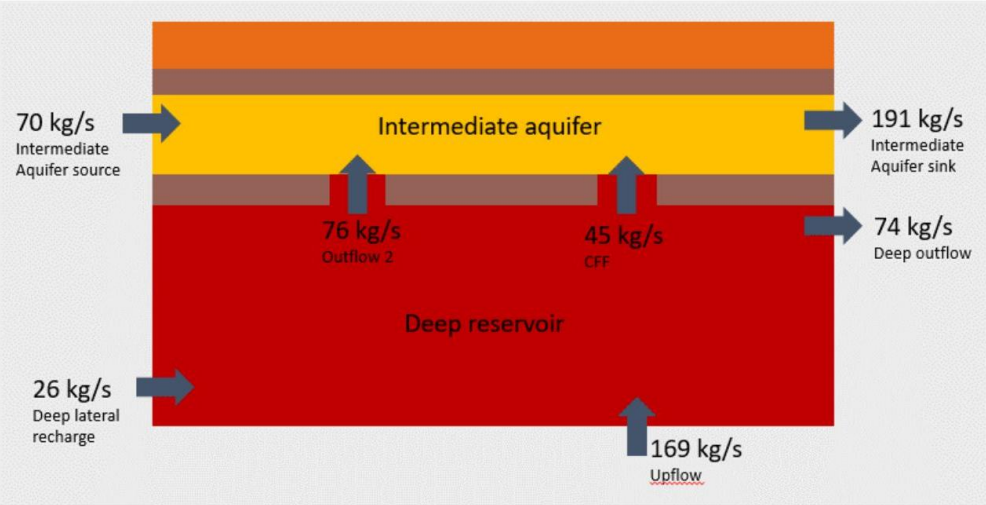


Figure 1: Simulated mass balance of the intermediate aquifer in the natural state (not to scale). Outflow refers to the natural percolation, and CFF refers to the central field fault.

A low level of combined brine fluid has been reinjected into the intermediate aquifer since commissioning as a corrosion mitigation strategy for the nearby external well casings. The combined brine refers to mixed brine and condensate from the binary plant. The mechanism was thought to primarily dilute the naturally occurring corrosive fluid. However, wall thickness surveys conducted since 2015 noted external metal loss on a small number of carbon steel casings around the intermediate aquifer. This suggests that corrosion in the area has continued, and it remains unclear whether the brine reinjection strategy has slowed or accelerated the corrosion rate. Reinjection could increase fluid corrosivity, as the combined brine fluid also contains dissolved CO_2 and may increase the partial pressure of CO_2 (P_{CO_2}) in the intermediate aquifer fluid.

This paper presents a study that models the corrosion thermodynamics and predicts the CO_2 corrosion rate of carbon steel casings in nearby wells exposed to a mixture of intermediate aquifer fluid. The main objective of this study is to investigate the effect of injecting combined brine fluid at different flow rates on the corrosivity of the final fluid mixture in the intermediate aquifer.

2 METHODOLOGY

The corrosion study described in this paper was carried out in three steps. The first step involved determining the high-temperature chemistry of the brine mixture at the intermediate aquifer temperature. The second step focused on constructing a Pourbaix diagram to predict the stability of corrosion products. The final step involved predicting CO_2 corrosion rates using models published by de Waard and Lotz (1994) and de Waard, Lotz, and Milliams (1991). The details of these three steps are further described in Sections 2.1 through 2.3.

2.1 Determination of the Corrosion Chemistry of the Fluid Mixture

From Figure 1, the intermediate aquifer water chemistry used was based on pre-modelled data for fluid percolating up from the deep reservoir at an aquifer pressure of 24.8 bar. The water chemistry of the intermediate aquifer was never directly sampled prior to shallow injection. The combined brine water chemistry used in this study represents a typical composition obtained at a sampling pressure of 14.4 bar and temperature of 137 °C. These water chemistries were then analyzed using the WATCH24 software, developed by Arnosson and Bjanrsason (1993), to model the chemical species present under high-temperature, single-phase conditions at different reinjection flow rates.

The chemistry model was calculated to determine the final intermediate aquifer conditions at 225 °C and at saturation pressure. This temperature was selected based on measured data from an abandoned well that was heated solely by the intermediate aquifer and is, therefore, considered representative of the aquifer's temperature in the area of interest. The chemistry was modelled under the assumption that the water composition was derived from rising water and steam laden with CO_2 gas from the deep reservoir, which reacted with local water to produce a CO_2-rich liquid phase.

Table 1 presents key chemistry data calculated using the WATCH24 software for mixtures of intermediate aquifer fluid and combined brine at different reinjection flow rates. The minimum historical reinjection rate was approximately 10 kg/s, while the maximum was approximately 80 kg/s. Table 1 shows the water chemistry output from WATCH24 for reinjection rates of 10 kg/s, 45 kg/s, and 80 kg/s, which correspond to 5 wt.%, 19 wt.%, and 30 wt.% dilution, respectively.

2.2 Construction of Pourbaix Diagrams to Predict Corrosion Product Stability

The WATCH24 chemistry outputs in Table 1 were then used as input data for constructing Pourbaix diagrams. An in-house software program based on the Electric Power Research Institute (EPRI) methodology developed by Chen and Aral (1983) was used, with a database that has been refined over the years. This database has proven effective for geothermal steam and brine environments in New Zealand, the Philippines, Indonesia, and Japan, as shown in published papers by Humphreys et al. (2015), and Lichti, Wilson, and Inman (1997).

The iron content in the intermediate aquifer was assumed to be very low for downhole geothermal fluids, at approximately 1.0×10^{-6} mol/kg. Pourbaix diagrams were prepared for the intermediate aquifer and for the condensate-intermediate aquifer mixture chemistries encountered at brine reinjection rates of 10 kg/s, 45 kg/s, and 80 kg/s.

Table 1. Key calculated data by WATCH24 software for intermediate aquifer, combined brine, and the mixtures

	Intermediate aquifer	Combined brine	Calculated brine and intermediate aquifer mix			Units
			Brine (10kg/s) + intermediate aquifer (191 kg/s)	Brine (45kg/s) + intermediate aquifer (191 kg/s)	Brine (80kg/s) + intermediate aquifer (191 kg/s)	
Temperature	225	22.5	225	225	225	°C
pH	5.10	5.70	5.12	5.17	5.21	
Species						
Cl^-	1.62E-02	2.01E-02	NC*	NC	NC	Mol/kg
SO_4^{2-}	6.76E-05	5.22E-06	NC	NC	NC	Mol/kg
HCO_3^-	7.57E-02	4.26E-04	NC	NC	NC	Mol/kg
HS^-	1.12E-03	1.00E-04	NC	NC	NC	Mol/kg
$SiO2_{(aq)}$	1.30E-02	1.97E-02	NC	NC	NC	Mol/kg
Ca^{2+}	1.54E-05	4.23E-05	NC	NC	NC	Mol/kg
K^+	2.76E-03	3.13E-03	NC	NC	NC	Mol/kg
Na^+	1.51E-02	1.17E-02	NC	NC	NC	Mol/kg
Total Fe	1.00E-06	3.39E-06	1.12E-06	1.46E-06	1.70E-06	Mol/kg
Total S	1.19E-03	9.02E-04	1.17E-03	1.12E-03	1.08E-03	Mol/kg
Total C	7.57E-02	4.57E-03	7.22E-02	6.21E-02	5.47E-02	Mol/kg
pCO_2	6.90E+00	4.30E-01	6.60E+00	5.60E+00	5.00E+00	Bar
PH_2	3.20E-01	NM*	3.20E-01	3.20E-01	3.20E-01	Bar
PH_2S	2.00E-02	2.85E-03	1.90E-02	1.70E-02	1.50E-02	Bar

* NC refers to not calculated and NM refers to not measured.

2.3 Prediction of CO2 Corrosion Rates

De Waard and Lotz (1994) recommended two correction factors for calculating the corrosion rate of carbon steel controlled by dissolved CO_2. These correction factors account for the effects of corrosion product scaling—either $FeCO_3$ or Fe_3O_4 dominant—and the influence of pH when Fe^{2+} ions is saturated at different temperatures. Since H_2S is present in the fluid, an additional correction factor was applied to account for its effect, based on published studies by Humphreys et al. (2015) and Lee (2004), which reported CO_2 corrosion in H_2S environments at elevated temperatures of approximately 120 °C. Based on the available data in Lee (2004); Smith and Pacheco (2002); and Kvarekval, Nyborg, and Choi (2003), the calculated correction factor decreases when the temperature increases up to 120 °C. Therefore, using the correction factor for the effect of H_2S at 120 °C in this case (225 °C) is considered conservative.

3 RESULTS AND DISCUSSIONS

3.1 Pourbaix Diagrams for the Prediction of Corrosion Product Stability

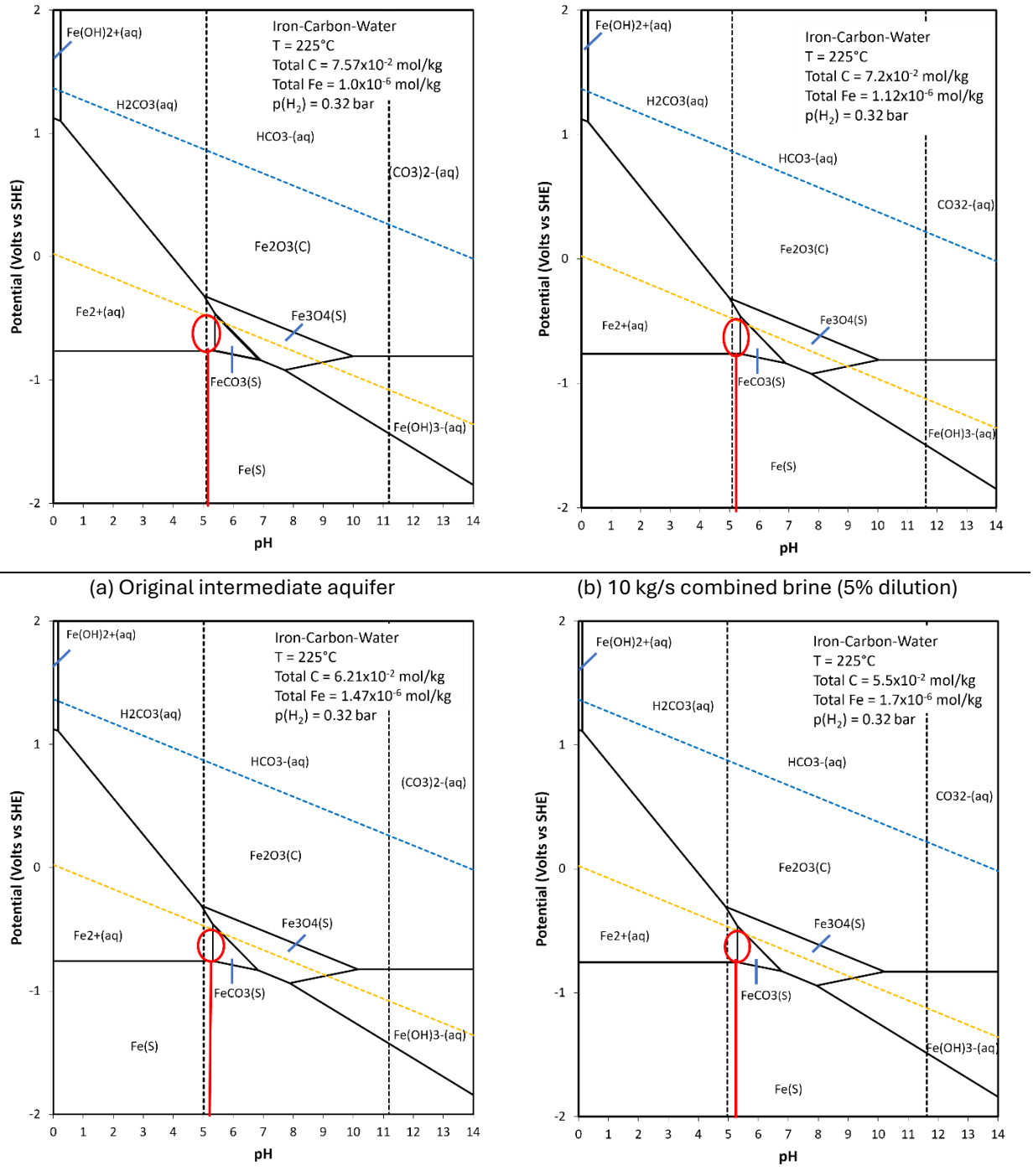
Separate Pourbaix diagrams were prepared for the Fe–CO_2–H_2O and Fe–H_2S–H_2O systems. In combination, even very small concentrations of H_2S are sufficient to suppress the stability of $FeCO_3$. However, it is important to assess the potential stability region of $FeCO_3$, as it forms a poorly protective corrosion product.

Figure 2 presents the Pourbaix diagram for the Fe–CO_2–H_2O system at 225 °C under different reinjection rates. The figure indicates that CO_2 corrosion reactions are predicted to occur in the absence of H_2S across all reinjection rates considered, due to the reaction of casing steel with CO_2 and H_2O to form $FeCO_3$, as described by Reaction (1).

$$Fe + CO_2 + H_2O \rightarrow FeCO_3 + H_2 \quad (1)$$

CO_2 corrosion was confirmed in a corroded well casing sample exposed to the intermediate aquifer, which experienced casing failure in 2003. However, analysis of the casing sample revealed repeating layers of Fe_3O_4 corrosion product and void spaces, as reported by Prabowo et al. (2023). Ikeda and Ueda (1994) also identified

Fe_3O_4 as the dominant phase in the corrosion products of carbon steel exposed at a P_{CO_2} of 3.8 bar, pH 4, and 200 °C. Prabowo et al. (2023) provided an equilibrium diagram for the reaction between Fe_3O_4 and $FeCO_3$. Their diagram showed that the stability region for Fe_3O_4 dominance at intermediate aquifer conditions (P_{CO_2} = 6.9 bar at 225 °C) begins at a hydrogen partial pressure (P_{H_2}) of 0.1 bar and increases with decreasing P_{H_2}. This condition suggests possible formation of Fe_3O_4 in the absence of H_2S.



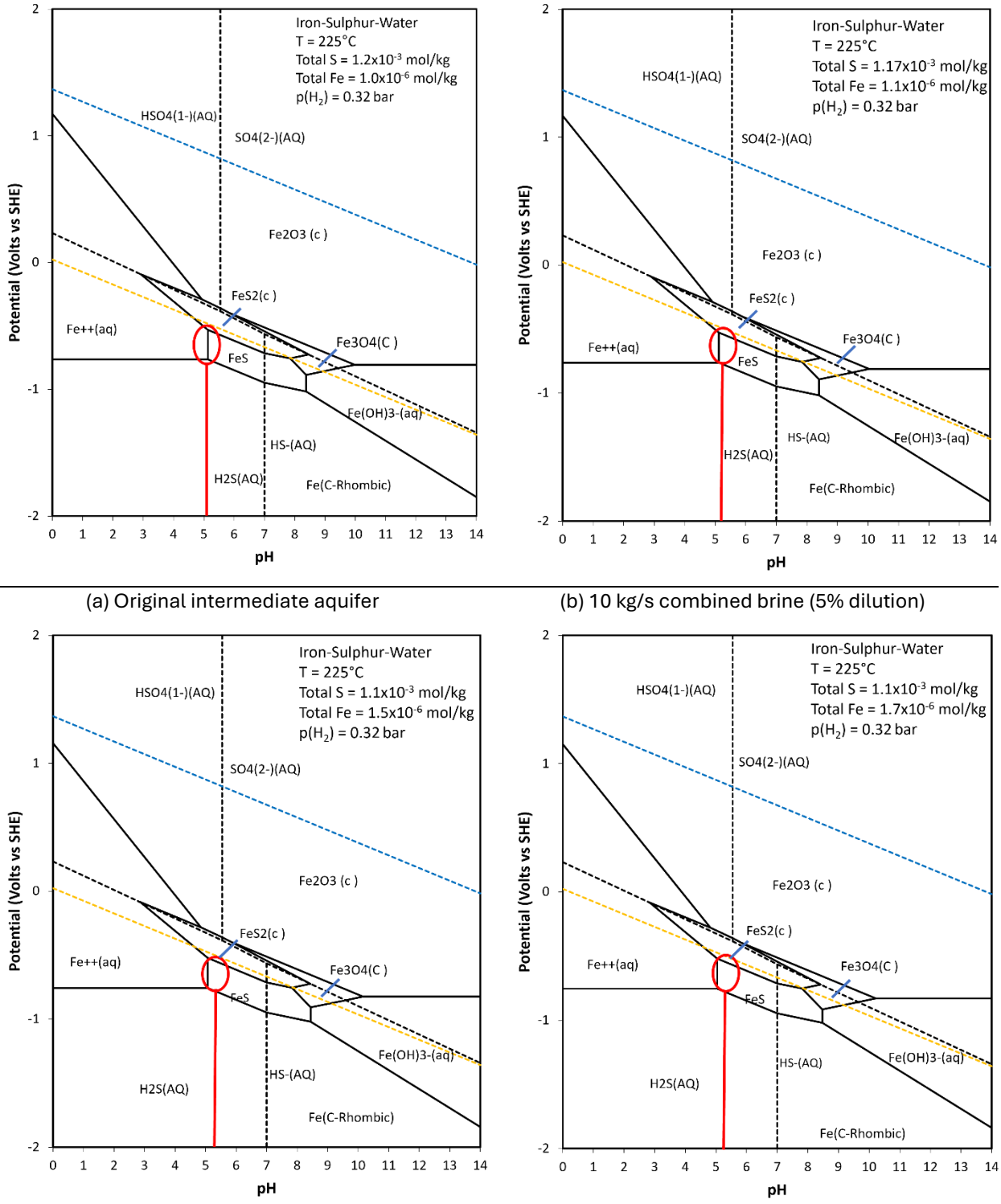
(a) Original intermediate aquifer (b) 10 kg/s combined brine (5% dilution)

(c) 45 kg/s combined brine (19% dilution) (d) 80 kg/s combined brine (30% dilution)

Figure 2. Potential-pH Pourbaix Fe-CO_2-H_2O diagrams for different reinjection rates at 225 °C. Dashed blue line is oxygen line. Dashed orange line is hydrogen line.

Figure 3 shows the Pourbaix diagram for the Fe–H_2S–H_2O system at 225 °C under different reinjection rates. The diagram indicates that the condition for the intermediate aquifer (marked by red circles in Figure 3) lies around the equilibrium line between Fe^{2+} (free corrosion) and FeS/FeS_2 (iron sulfide formation). This suggests a potential competition among three corrosion pathways: free corrosion forming Fe^{2+} under acidic pH, CO_2 corrosion forming iron carbonate ($FeCO_3$), and iron sulfide formation stabilized by increased iron content at the surface. Given that Fe_3O_4 corrosion products are intermittently formed, another possible scenario involves partial

shielding of the casing surface by a thin layer of iron carbonate. This layer may reduce H_2S access to the surface, allowing the formation of iron oxide, as discussed in the published work by Ghaziof et al. (2017). With increasing reinjection rates, Fe^{2+} concentration and pH slightly increase, while CO_2 is diluted and total sulfur changes only marginally. This results in a slight shift in corrosion conditions toward the formation of FeS/FeS_2. These findings support the application of both iron sulfide scaling models and CO_2 corrosion models for predicting corrosion rates.



(a) Original intermediate aquifer

(b) 10 kg/s combined brine (5% dilution)

(c) 45 kg/s combined brine (19% dilution)

(d) 80 kg/s combined brine (30% dilution)

Figure 3. Potential-pH Pourbaix Fe-H_2S-H_2O diagrams for different reinjection rates at 225 °C. Dashed blue line is oxygen line. Dashed orange line is hydrogen line.

3.2 Prediction of Corrosion Rate

The Pourbaix diagrams shown in Figure 2 and Figure 3 indicate a potential competition between free corrosion, CO_2 corrosion, and the formation of protective iron sulfide scaling. Therefore, the corrosion rate prediction was calculated using four corrosion factors across four scenarios. Figure 4 and Figure 5 show the calculated CO_2 corrosion rates of carbon steel at different temperatures, with reinjection rates of 10 kg/s (low rate) and 80 kg/s (highest historical rate). The worst-case scenario assumes the absence of H_2S, while the best-case scenario assumes dominant H_2S effects, leading to the formation of protective iron sulfide scaling. Although the Pourbaix diagrams show a slight shift in corrosion conditions, the predicted corrosion rates for the two reinjection patterns are broadly similar. This is because pH and P_{CO_2}, which are the key controlling chemical parameters, do not change significantly with variations in brine reinjection rate, contrary to initial concerns about a potential increase in P_{CO_2} due to brine reinjection.

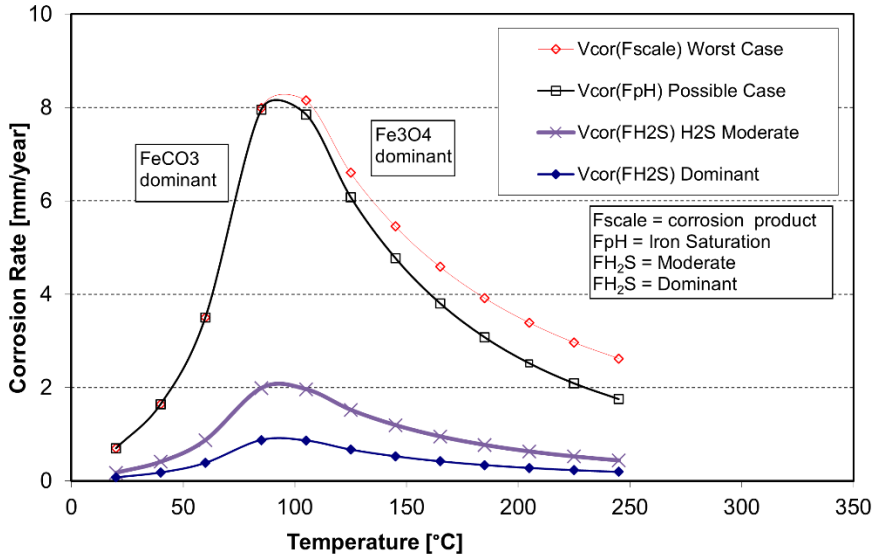


Figure 4: Calculated CO_2 corrosion rate for the 10 kg/s combined brine + intermediate aquifer (5% dilution).

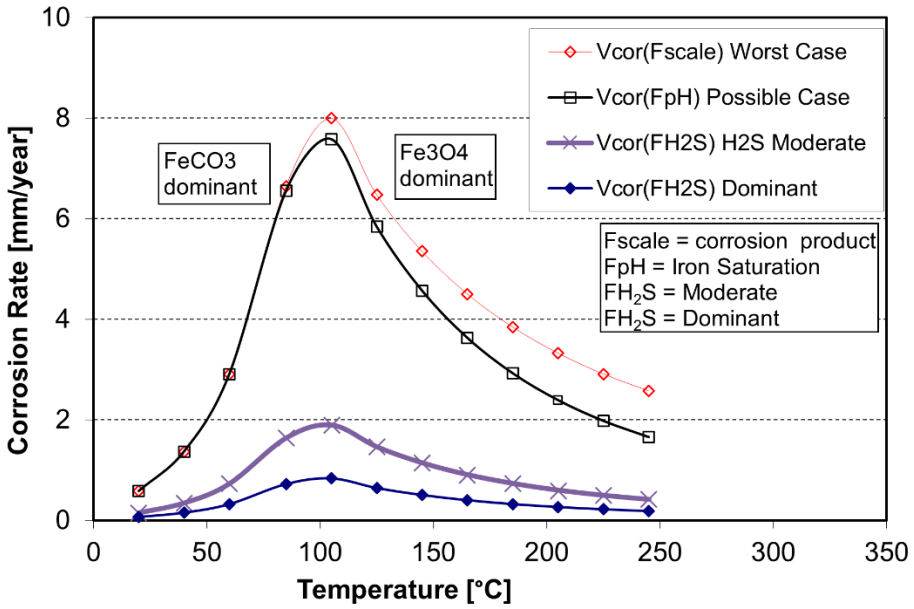


Figure 5: Calculated CO2 corrosion rate for the 80 kg/s combined brine + intermediate aquifer (30% dilution).

The predicted corrosion rates increase with temperature from ambient up to 100 °C but then decrease as temperature rises further, as shown in Figure 4 and Figure 5. At temperatures up to 100 °C, CO_2 corrosion (Reaction [1]) is dominant, and the corrosion rate is strongly dependent on temperature due to the higher

thermodynamic driving force, as modeled by de Waard, Lotz, and Milliams (1991). At temperatures above 100 °C, Fe_3O_4 begins to form, and its stability increases with rising temperature, also as modeled by de Waard, Lotz, and Milliams (1991). Fe_3O_4 is a protective corrosion product because it is denser and more adherent than $FeCO_3$. As a result, the corrosion rate decreases with increasing temperatures beyond 100 °C.

The predicted corrosion rates depend on the formation of iron sulfide scaling. At the temperature of the intermediate aquifer (225 °C), the predicted corrosion rate under the worst-case scenario, where no H_2S is present and only scaling by the poorly protective $FeCO_3$ corrosion product occurs, is approximately 3 mm/year. Since H_2S is present in both the intermediate aquifer and the combined brine mixture, there is potential for iron sulfide scaling to form. At a moderate effect of H_2S scaling, a reduced corrosion rate of approximately 0.5 mm/year is predicted. In the best-case scenario, where iron sulfide scaling is dominant, the corrosion rate is expected to be as low as approximately 0.2 mm/year. It is important to note that the consideration of the effect of H_2S for the formation of iron sulfides only when elevated iron is available in solution and significant level of H_2S is present.

4 CONCLUSIONS

The impact of reinjecting combined brine on the corrosion rate of carbon steel well casings located within the intermediate aquifer has been modelled. CO_2 corrosion reactions are predicted to occur under all reinjection rates into the intermediate aquifer. Historical observations of casing corrosion in the aquifer suggest that CO_2 corrosion has occurred, accompanied by intermittent formation of Fe_3O_4.

The Fe–H_2S–H_2O Pourbaix diagrams show that the mixed fluid chemistry lies around the equilibrium line between Fe^{2+} and iron sulfides. This suggests a potential competition between free corrosion forming Fe^{2+} under acidic pH, CO_2 corrosion, and the formation of iron sulfides. The predicted CO_2 corrosion rate of carbon steel at 225 °C and pH 5.1, with a moderate level of H_2S, ranges from approximately 0.2 to 3 mm/year depending on the influence of H_2S. The highest predicted corrosion rate, around 3 mm/year, corresponds to the worst-case scenario of the absence of H_2S and no iron saturation. The lowest rate, approximately 0.2 mm/year, occurs when H_2S scaling (i.e., formation of iron sulfide scale) is dominant and effectively mitigates CO_2 corrosion.

One aspect not addressed in this paper is the effect of temperature variation in wells located at different distances from the intermediate aquifer. Pourbaix diagrams and corrosion rates should be modelled at each specific temperature. This has important implications, as CO_2 corrosion may be more prevalent at lower temperatures where H_2S scaling is less dominant. A reassessment of casing wall loss across wells operating under varying temperature conditions is necessary to better quantify corrosion rates and associated risks.

Acknowledgements

The authors wish to thank Rotokawa Joint Venture Limited, Mercury New Zealand Limited, and Quest Integrity for the permission to publish this paper.

REFERENCES

Arnosson, S., and Bjanrsason, J. O.: WATCH (1993) https://en.isor.is/software/.

Chen, C.M., and Aral, K.: Computer-Calculated Potential PH Diagrams to 300°C, EPRI NP-3137 Project 1167-2 (1983), Electric Power Research Institute.

de Waard, C., and Lotz, U.: Prediction of CO_2 Corrosion of Carbon Steel, In A Working Party Report on Predicting CO2 Corrosion in Oil and Gas Industry, *European Federation of Corrosion Publications*, **13**, (1994), 30-49.

de Waard, C., Lotz, U., and Milliams, D. E.: Predictive Model for CO_2 Corrosion in Wet Natural Gas Pipelines, *Corrosion*, **47**, (1991), 976-985

Ghaziof, S., Dudley, R., Julian, K., Ko, M., Lichti, K. A.: H_2S Corrosion of Carbon Steel in Geothermal Fluids, Proceedings 39th New Zealand Geothermal Workshop 2017, Energy Events Centre, Rotorua, New Zealand (2017).

Humphreys, B., Christoffersen, C. Lichti, K. A., Wong, J., Ko, M., and Dudley, R.: Corrosion and Scaling in Habanero 4 Produced Fluids and 1 MWe Demonstration Plant, Proceedings World Geothermal Congress 2015, Melbourne Convention and Exhibition Centre, Melbourne, Australia (2015).

Ikeda, A., and Ueda, M.: CO_2 Corrosion Behavior of Cr-Containing Steels, In A Working Party Report on Predicting CO2 Corrosion in Oil and Gas Industry, *European Federation of Corrosion Publication*, **13**, (1994), 59–93.

Kvarekval, J., Nyborg, R., and Choi, H.: Formation of Multilayer Iron Sulfide Films During High Temperature CO_2/H_2S Corrosion of Carbon Steel, NACE Corrosion Proceeding, Sandiego Convention Centre, San Diego, United States (2003).

Lee, K. J.: A Mechanistic Modelling of CO_2 Corrosion of Mild Steel in the Presence of H2S. Doctoral Thesis, Department of Chemical Engineering, Ohio University (2004).

Lichti, K. A., Wilson, P. T., Inman, M. E., Corrosivity of Kawerau Geothermal Steam, *Geothermal Resources Council Transactions*, **21**, (1997), 25-32.

Prabowo, S., Young, A., Lichti, K. A., Melia, K., Calibugan, A., and Siega, F.: Corrosion Risk Assessment for Reinjection of Aerated Condensate, Proceeding of AMPP CONFERENCE, Colorado Convention Center, Denver, United States (2023).

Smit, S., and Pacheco, J.: Prediction of Corrosion in Slightly Sour Environments, NACE Corrosion Proceeding, NACE Corrosion Proceeding, Colorado Convention Center, Denver, United States (2002).